30th International Congress on Sound and Vibration

ICSV30 AMSTERDAM 8-11 JULY 2024

AN AXISYMMETRIC MODEL FOR PREDICTING TURBULENT FLOW NOISE IN TOWED SONAR ARRAYS

Rakesh Sekharipuram Sekar, Ganesh Natarajan, Pramod Kuntikana and Anoop Akkoorath Mana*

Department of Mechanical Engineering, Indian Institute of Technology Palakkad, India, 678623

**E-mail: akkoorath@iitpkd.ac.in*

Towed sonar arrays house a series of pressure sensors inside a fluid-filled elastic tube. Towing of the sonar array in water generates a turbulent boundary layer on the exterior surface of the fluid-filled elastic tube. The pressure fluctuations in the turbulent boundary layer along with other ambient pressure fluctuations, excites the elastic tube and further generates pressure disturbances in the interior fluid. An empirical model proposed by Chase is widely used for predicting the turbulent pressure spectrum for an axial flow past a cylinder. However, predictions using the Chase model show large deviation from existing experimental results at low tow speeds. In this work we propose a "hybrid" model derived using the insights gained from the Chase empirical model. The new hybrid model predicts a turbulent pressure spectrum that shows closer agreement with the experimental results for an axial flow over a cylinder at all tow speeds. The exterior turbulent pressure field generates pressure fluctuations in the interior fluid (flow noise) that are modeled using the linear acoustic theory. In this work, we also present an axisymmetric vibroacoustic model to predict the interior on-axis sound pressure level. The vibroacoustic model is fully coupled as it combines the vibrations in the elastic tube (using the Navier-Lame equations) with the pressure field in the interior fluid. We employ the new hybrid model in conjunction with the vibroacoustic model to estimate the on-axis sound pressure level due to the exterior turbulent pressure excitations at different tow speeds and elastic tube diameters. Our results show that while the flow noise increases with tow speed, the change in elastic tube diameter influences the noise spectrum only at relatively high frequencies. This work is supported by the Deference Research and Development Organization, India.

Keywords: turbulent flow noise, sonar array, fluid-filled elastic tube, fully coupled vibroacoustic model

1. Introduction

Towed sonar arrays house a series of pressure sensors inside a fluid-filled elastic tube. Towing of sonar array in water generates a thick layer of turbulent flow over the exterior surface of the fluid-filled elastic tube. The pressure fluctuations in the turbulent boundary layer (TBL) along with other ambient sea pressure fluctuations, excites the elastic tube and further generates acoustic pressure disturbances in the interior fluid. The hydrophones placed in the interior fluid picks these acoustic signals. The signals associated with the turbulent pressure fluctuations are called flow noise. Currently, the flow noise is measured either by towing the sonar array in open water using a dinghy or by allowing the hydrophone to free fall in water[1]. In the first case, noise from the boat and vibrations of the towline connections

pollutes the measured acoustic signals[2]; whereas in the second case, the useful measurements can be made only at the terminal velocity of the hydrophone. This work aims at developing a numerical model for predicting the flow noise in thin (length to radius ratio of the elastic tube greater than 1000) towed sonar arrays which is useful over wide range of towing speeds.

2. Semi-empirical models for turbulent pressure spectrum

Of the several models, the one by Chase [3] is widely used to predict the turbulent pressure field for an axial flow past a solid cylinder.

2.1 Chase model

Chase initially proposed a model for predicting turbulent pressure spectrum over a flat plate [3]:

$$P(k_z, k_2, \omega) = C_2 \rho^2 v_*^6 \omega^{-3} (v_* K/\omega)^2 \tag{1}$$

where $K^2 = k_z^2 + k_2^2$, k_z and k_2 are the wavenumbers in the direction of flow (axial) and cross flow, respectively. ω denotes the frequency, ρ the density of the fluid and $\nu_* = 0.04U$ is the friction velocity with U representing the free stream velocity. Chase[3] further derived the turbulent pressure spectrum for an axial flow past a solid cylinder by incorporating the azimuthal variations as given by

$$P_m(k_z, \omega) = \int_{(m-1/2)/R}^{(m+1/2)/R} P(k_z, k_2, \omega) dk_2 \tag{2}$$

Here, m is a whole number associated with the azimuthal variation and R is the radius of the cylinder.

For an axisymmetric flow ($m = 0$), the above integral yields, after including correction terms for the convective wavenumber,

$$P_0(k_z, \omega) = C\rho^2 \nu_*^3 R^2 \left[(k_z R)^2 + \frac{1}{12}\right] \left[\frac{(\omega R - u_c k_z R)^2}{h^2 \nu_*^2} + (k_z R)^2 + b^{-2}\right]^{-2.5} \tag{3}$$

In the above equation, u_c denotes the convective speed ($u_c = 0.68U$, a large fraction of tow speed U), $C = 0.063$ and $h = 3.7$. Although the above model predicts the spectrum at low frequencies fairly well, the estimated values are very small compared to experiments [2], particularly at low tow speeds.

2.2 Frendi model

Another important turbulent pressure spectrum model for flow over flat plate is that by Frendi et al. [4]. Frendi et al. proposed that the turbulent pressure field over a flat plate is given by

$$\hat{R}(k_z, k_2, \omega) = C_1 R^*(\omega) e^{-\hat{\alpha} r_k} \tag{4}$$

where $R^*(\omega)$ is turbulent pressure field autospectrum [5], C_1 is constant, $\hat{\alpha}$ is given by $\hat{\alpha} = \alpha\delta$ where α is a constant, δ is the boundary layer thickness[4], r_k depends of the axial wavenumber (k_z) and cross flow wavenumber (k_2) given by [4]

$$|r_k^2| = (k_z - \frac{\omega}{u_c})^2 + (mk_2)^2 \tag{5}$$

In the above equation, m is the scaling factor which is approximately taken as 1/7.7 [4], ω is the frequency and u_c is the convective speed. The term α is given by [4]

$$\alpha = \frac{a_1}{\pi} \frac{1}{\sqrt{1 + a_2(\frac{\omega\delta}{u_t} - 50)^2}} \tag{6}$$

where u_t (v_* in Chase model) is the friction velocity, $a_1 = 4.7$ and $a_2 = 3e^{-5}$.

2.2.1 Modified Frendi model

The above Frendi's model (Eq. 4) can be modified to suit to the case of an axial flow past a solid cylinder using Eq. 2. Accordingly, the turbulent pressure wavenumber-frequency spectrum for a cylinder (axisymmetric) is thus given by

$$\hat{R}(k_z, \omega) = \int_{-1/2a}^{1/2a} \hat{R}(k_z, k_2, \omega) dk_2 \tag{7}$$

It is observed that the modified Frendi model overpredicts the turbulent flow noise for axial flow over a cylinder with respect to experimental observations [2].

3. A new hybrid model

In this section, we develop a "hybrid" model using the insights from the Chase and the Frendi models. The intent is to have a better model prediction closely matching with the experimental results of Unnikrishnan [2]. In the new hybrid model, we use the pressure spectrum of Chase and an exponential decay function of Frendi. The new hybrid model is given by

$$P(k_z, k_2, \omega) = C_3 \bar{P}(\omega) e^{-\hat{\alpha} r_k} \tag{8}$$

Here $C_3 = 0.0001$ and the pressure spectrum $\bar{P}(\omega)$ is obtained by integrating the turbulent pressure field proposed by Chase (see Eq. 3) over the axial wavenumber k_z:

$$\bar{P}(\omega) = \int_{-\infty}^{\infty} P_0(\omega, k_z) dk_z \tag{9}$$

The term $\hat{\alpha} = \alpha\delta$, where α is given by Eq. 6. a_1 determines the shape of the flow noise at low frequencies and a_2 determines the shape at high frequencies. We used $a_2 = 3e^{-6}$ and tried different a_1 values to match the Unnikrishnan's experiment results. $a_1 = 1$ gives a better match with the experimental results.

3.1 Flow noise

The flow noise measured by an array of hydrophones is given by [2]

$$Q(\omega) = \int_{-\infty}^{\infty} P(k_z, \omega) H(k_z) dk_z \tag{10}$$

In the above equation, $P(k_z, \omega)$ is the wavenumber frequency spectrum of turbulent pressure field as received by a single hydrophone and $H(k_z)$ is the hydrophone response function. The hydrophone array

is a set of large number of similar elements with specific length arranged at a fixed distance apart. This array acts as noise filter and its response (hydrophone response function) is given by [2]

$$H(k_z) = \frac{sin(k_z dN/2)}{N sin(k_z d/2)} \frac{sin(lk_z/2)}{lk_z/2} \tag{11}$$

where N is the number of small elements in the array, d is the distance between two elements and l is the length of individual elements. For the new hybrid model, the flow noise is given by

$$Q(\omega) = \int_{-\infty}^{\infty} \int_{-1/2a}^{1/2a} C_3 \bar{P}(\omega) e^{-\hat{\alpha} r_k} H(k_z) dk_2 dk_z \tag{12}$$

A comparison of flow noise computed using the hybrid model, Chase model [3], modified Frendi model [4] and Unnikrishnan's experiment [2] are shown in Fig. 1. The experiment reported in [2] was conducted in a quiet lake with the help of a dinghy pulled by a hydraulic winch to reduce the noise from propulsion systems. However, the measured flow noise levels beyond 400 Hz was limited by the ambient noise floor. This indicates the presence of ambient noise in the results presented in [2]. It can be observed from Fig. 1 that the Chase model predictions are comparable with respect to the measured values [2] at high towing speeds. But, the deviation is large at higher frequencies for low tow speeds. It can be observed that the modified Frendi model [4] is over predicting the flow noise at almost all the frequencies. At all tow speeds, the new hybrid model predictions are closer to the measured values [2] than the Chase model and the modified Frendi model predictions.

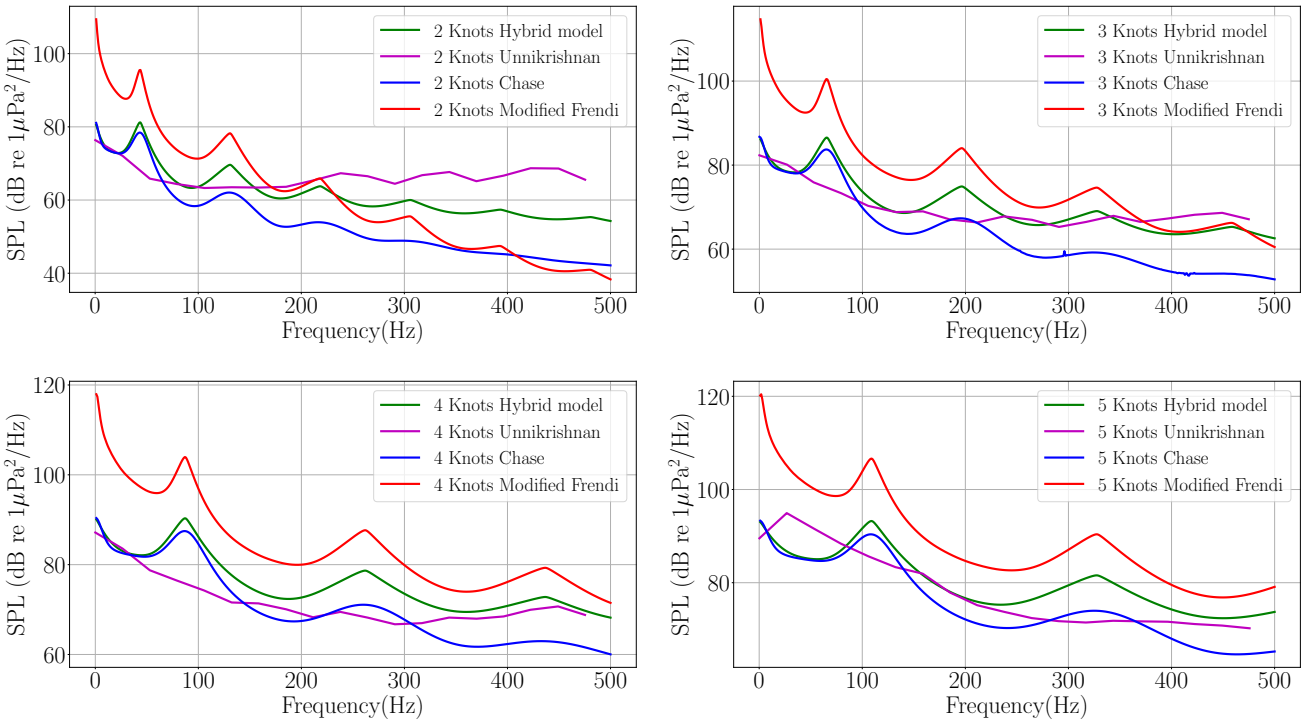

Figure 1: A comparison of flow noise predicted by the hybrid model, the Chase [3] model and modified Frendi model [4] with that measured from experiments [2].

The non-dimensional power spectral density calculated using the new hybrid model for different tow speeds are shown in Fig. 2. The non-dimensional power spectral density for different tow speeds collapse

to a single curve against the non-dimensional frequency space $\omega D/U$. One can obtain the power spectral density at different tow speeds and cylinder diameters using this “single" non-dimensional curve.

A comparison of wavenumber frequency pressure spectrum for the hybrid, the Chase and the modified Frendi models at 2 Knots is shown in Fig. 3. It can be seen that for all models, the spectrum peaks at convective wavenumber and it further reduces with wavenumber. The hybrid model and the modified Frendi model pressure spectrum reduces at a faster rate beyond the convective wavenumber than the Chase model.

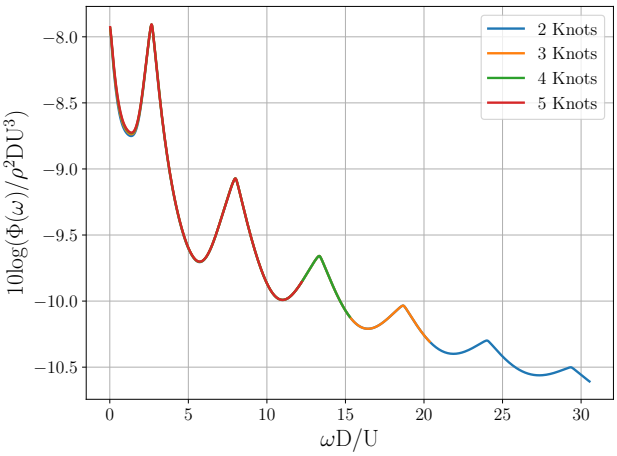

Figure 2: Non-dimensional power spectral density for different tow speeds using the new hybrid model.

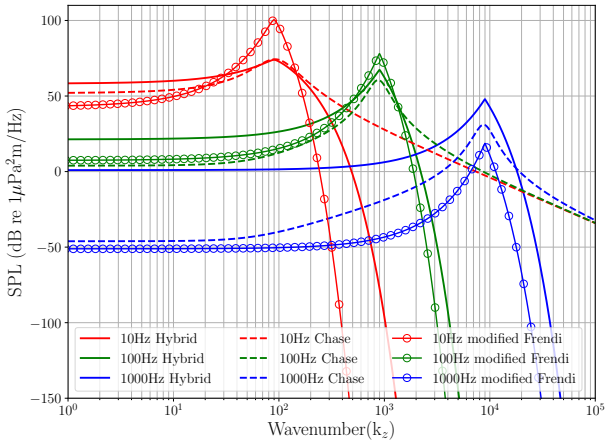

Figure 3: A comparison of turbulent pressure spectrum of the hybrid model with the modified Frendi and the Chase models.

4. Axisymmetric vibroacoustic model of a fluid-filled elastic tube

The turbulent pressure field excitation at the exterior creates vibrations in the elastic tube which in turn generates acoustic pressure fluctuations in the interior fluid where the hydrophone array is placed. In this section, we develop an axisymmetric model of the fluid-filled elastic tube and use it to calculate the sound pressure level received by the hydrophone array.

The elastic tube may be modeled using the Navier-Lame equations [6]

$$\mu\nabla^2\underline{\mathbf{u}} + (\lambda+\mu)\nabla\nabla.\underline{\mathbf{u}} = \rho\ddot{\underline{\mathbf{u}}} \tag{13}$$

where λ and μ are the Lame’s constants, $\underline{\mathbf{u}}$ is the displacement vector and ρ is the density of the tube.

4.1 Elastic tube displacement and stress components

Transforming the above equation into the Fourier domain and solving for the axial (U_e) and the radial (W_e) displacements, we get [6]

$$\hat{W}_e(r,k_z,\omega) = (\hat{Q}_1 J_1(r\beta_1) + \hat{R}_1 Y_1(r\beta_1))\chi_1 + (\hat{Q}_2 J_1(r\beta_2) + \hat{R}_2 Y_1(r\beta_2))\chi_2 \tag{14}$$

$$\hat{U}_e(r,k_z,\omega) = \hat{Q}_1 J_0(r\beta_1) + \hat{R}_1 Y_0(r\beta_1) + \hat{Q}_2 J_0(r\beta_2) + \hat{R}_2 Y_0(r\beta_2) \tag{15}$$

$$\beta_1^2 = \frac{\omega^2}{C_L^2} - k_z^2,\ \beta_2^2 = \frac{\omega^2}{C_T^2} - k_z^2,\ C_L^2 = \frac{\lambda+2\mu}{\rho} \text{ and } C_T^2 = \frac{\mu}{\rho}$$

The stress components can be derived using

$$\hat{\sigma_{rr}}(r, k_z, \omega) = (\lambda + 2\mu) \frac{\partial \hat{W}_e}{\partial r} + \frac{\lambda}{r} \left(\hat{W}_e \right) + \lambda \frac{\partial \hat{U}_e}{\partial z} \tag{16}$$

$$\hat{\tau_{rz}}(r, k_z, \omega) = \mu \left(\frac{\partial \hat{W}_e}{\partial z} + \frac{\partial \hat{U}_e}{\partial r} \right) \tag{17}$$

4.2 Acoustic pressure field inside the tube

The acoustic pressure field inside the elastic tube may be modelled using the acoustic wave equation

$$\nabla^2 P = \frac{1}{c^2} \frac{\partial^2 P}{\partial t^2} \tag{18}$$

where $P = P_f$ is the pressure inside the cylinder and c is the speed of sound in the fluid. Taking the Fourier transform and solving using the variable separable method we get

$$\hat{P}_f(r, k_z, \omega) = \hat{P}_i(k_z, \omega) J_0(\alpha r) \tag{19}$$

Using the Euler equation ($\nabla P_f = -\rho \frac{\partial u}{\partial t}$ where ρ is the density of the inside fluid and u is the velocity of the fluid inside the cylinder), the radial fluid displacement inside the fluid can be obtained as

$$\hat{U}_f(r, k_z, \omega) = -\hat{P}_i(k_z, \omega) \frac{\alpha}{\rho \omega^2} J_1(\alpha r) \tag{20}$$

where $\alpha = k_w^2 - k_z^2$, k_w $(= \omega/c)$ is the acoustic wavenumber.

4.3 Boundary conditions

The boundary conditions for fluid-filled elastic tube excited with an external turbulent pressure fields are given below.

1. The shear stress on the r plane in the z direction inside and outside of the tube is zero.

$$\tau_{rz}(b, k_z, \omega) = 0, \tau_{rz}(a, k_z, \omega) = 0 \tag{21}$$

   where b and a are the outer and inner radius of the tube, respectively.
2. On the outer surface of the elastic cylinder, normal stress is equal to the pressure due to the turbulent boundary layer.

$$\tau_{rr}(b, k_z, \omega) = -P_0(k_z, \omega) \tag{22}$$

   where $P_0(k_z, \omega)$ is the wavenumber-frequency spectrum of the turbulent pressure field. (For the Chase model, it is given by Eq. 3).
3. At the inside interface, the pressure inside the fluid is equal to the radial component of normal stress in the elastic tube.

$$P_f(a, k_z, \omega) = -\tau_{rr}(a, k_z, \omega) \tag{23}$$

4. The radial displacement of the fluid inside is equal to that in the elastic cylinder at the inside boundary.

$$U_f(a, k_z, \omega) = U_e(a, k_z, \omega) \tag{24}$$

These boundary conditions can be expressed in a matrix form and can be solved for the constant coefficients (Q_1, Q_2, R_1 and R_2) and $\hat{P}_i(k_z, \omega)$. Further we solve Eq. 19 for the inside pressure pressure field. Note that r can be varied to find the pressure at different location inside the tube.

4.4 Flow noise inside the fluid-filled elastic tube

The flow noise inside the tube is defined as [7]

$$Q(\omega) = 4\pi \int_{-\infty}^{\infty} |P_f(r, k_z, \omega)||H(k_z)|^2 dk_z \tag{25}$$

where $P_f(r, k_z, \omega)$ is the pressure field inside the fluid-filled elastic tube and $H(k_z)$ is the hydrophone response function (Eq. 11). The interior pressure field $P_f(r, k_z, \omega)$ may be considered as the product of the turbulent pressure outside and the tube transfer function.

Fig. 4 shows a comparison of the on-axis flow noise computed using the present model (combining the hybrid model for the turbulent pressure field and the axisymmetric vibroacoustic model for the fluid-filled elastic tube) with that of Jineesh et al. [8]. Table 1 lists the parameter values used to compute the flow noise. It can be seen that the present model predicts lower sound pressure levels at low frequencies ($\leq$ 10 dB) than that by Jineesh et al. Whereas at high frequencies, the present model predictions are higher ($\leq$ 10 dB) than Jineesh's predictions.

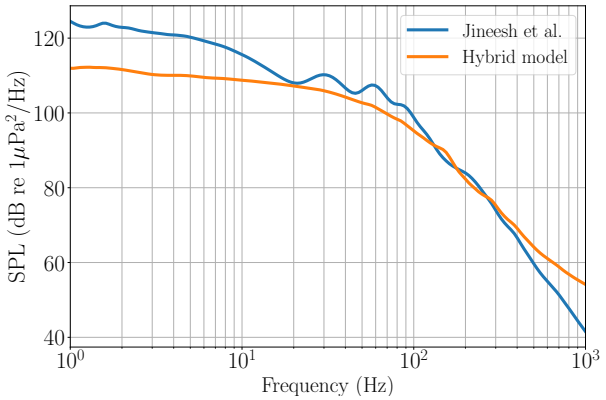

Figure 4: A comparison of the present model on-axis flow noise predictions with that of Jineesh et al. [8].

Table 1: Parameters used for estimation of flow noise inside the fluid-filled elastic tube.

Property	**Values**
Tube diameter (m)	0.04
Tube thickness (m)	0.005
Flow velocity (knots)	20
Number of hydrophones	50
Length of hydrophone (m)	0.05
Hydrophone spacing (m)	0.25
Exterior fluid density (kg/m^3)	1000
Interior fluid density (kg/m^3)	800
Reference pressure (μ Pa)	1

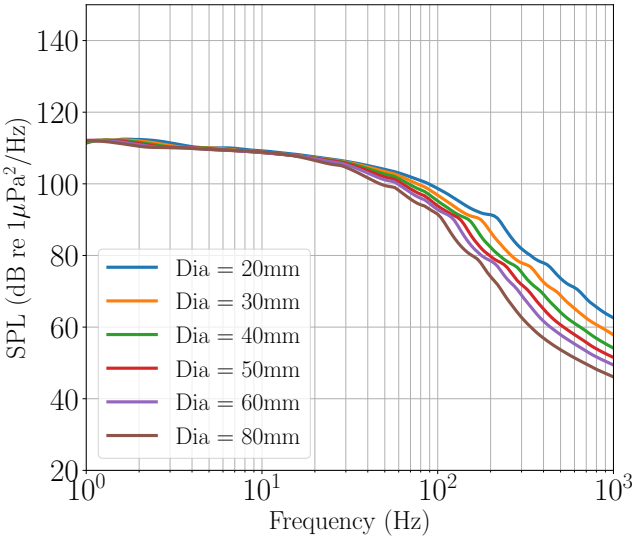

Figure 5: Flow noise variation with frequency for different (outside) tube diameters at 20 knots.

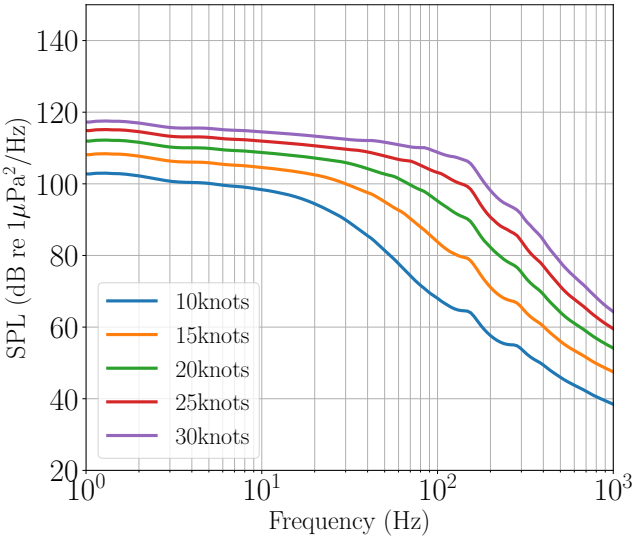

Figure 6: Flow noise variation with frequency at different speeds for a tube of outside diameter 40 mm.

The present model is further used to compute the on-axis flow noise for different tube diameters. Fig. 5 shows the variation in flow noise for six different (outside) diameters varying from 20 mm to 80 mm at 20 knots. There is hardly any change in the flow noise at lower frequencies. The corresponding radial wavelength at lower frequencies is much larger as compared to the tube diameters. Any attenuation due to an increase in diameter is therefore negligible at lower frequencies. However at high frequencies, the radial wavelength is comparable to the tube diameter. An increase in the tube diameter therefore results in an increase in the acoustic attenuation. This results in a lower sound pressure level for large diameter tubes at high frequencies. Fig. 6 shows the variation in on-axis flow noise for a tube of outside diameter 40 mm at different tow speeds. The turbulent pressure fluctuations increases in intensity with increasing tow speed. This results in an increased on-axis sound pressure level for higher tow speeds.

5. Conclusions

We have developed a new hybrid model for estimating the turbulent pressure field wavenumber-frequency spectrum for the axial flow past a solid cylinder of circular cross-section. The model predictions are found to be superior to that from a widely-used semi-empirical model and compares reasonably well with available experimental results. A fully coupled vibroacoustic model (axisymmetric) is developed to predict the on-axis pressure field inside a fluid-filled elastic tube. The model is obtained by coupling the Navier Lame equations for the elastic tube with the wave equation for the interior fluid. The model is further used to estimate the on-axis sound pressure level due to the turbulent pressure excitation at the exterior of the tube. The hybrid model presented in this work is used for estimating the turbulent pressure field at different tow speeds and tube diameters. The on-axis sound pressure level variation is found to be negligible at low frequencies for different tube diameters. However, it decreases with an increase in the tube diameter. The model also predicts an increase in the on-axis sound pressure levels with an increase in the tow speed.

References

1. Gopi, S., Felix, V. P., Sebastian, S., Pallayil, V. & Kuselan, S. *In-situ non-acoustic noise measurement system for towed hydrophone array* in *2010 IEEE Instrumentation Measurement Technology Conference Proceedings* (2010), 913–916.
2. Unnikrishnan, K. C., Pallayil, V., Chitre, M. A. & Kuselan, S. *Estimated flow noise levels due to a thin line digital towed array* in *OCEANS 2011 IEEE - Spain* (2011), 1–4.
3. Chase, D. M. *Further modeling of turbulent wall pressure on a cylinder and its scaling with diameter* Dec. 1981.
4. Frendi, A. & Zhang, M. A new turbulent wall-pressure fluctuation model for fluid–structure interaction. *Journal of Vibration and Acoustics* **142,** 021018 (2020).
5. Goody, M. Empirical spectral model of surface pressure fluctuations. *AIAA journal* **42,** 1788–1794 (2004).
6. Achenbach, J. *Wave propagation in elastic solids* (Elsevier, 2012).
7. Knight, A. Flow noise calculations for extended hydrophones in fluid-and solid-filled towed arrays. *The Journal of the Acoustical Society of America* **100,** 245–251 (1996).
8. Jineesh, G. & Ebenezer, D. D. *Response of a linear array of hydrophones to flow-induced noise* in *Acoustics* (2013), 1–6.